Explicit expressions for the dynamic polarization behavior in ferroelectrics with symmetric/asymmetric electrical conductivity

C. K. Wong and C. H. Tsang
Department of Applied Physics, The Hong Kong Polytechnic University, Hong Kong, China

F. G. Shin
Department of Applied Physics, Materials Research Center and Center for Smart Materials, The Hong Kong Polytechnic University, Hong Kong, China

(Received 3 February 2004; accepted 10 April 2004)

We model the dynamic polarization behavior of ferroelectric films by an analytical approach. Using a parallelogramlike *P-E* hysteresis model, explicit expressions were obtained for describing the *D-E* loops of ferroelectric films as would be measured from a Sawyer-Tower circuit. By introducing the consideration of electrical conduction, resistive losses inflate the ferroelectric loop to some extent. In addition, an asymmetric conduction will result in polarization offsets with the magnitude and direction depending on the asymmetric conductivities of the materials. The inflated loop, as well as the offset phenomena, which have been observed experimentally [e.g., L. Zheng, C. Lin, W.-P. Xu, and M. Okuyama, J. Appl. Phys. **79**, 8634 (1996)], will be discussed by means of our modeled results. Some simple exact formulas have been derived and the effects of electric, dielectric, and ferroelectric parameters, as well as the applied field on the ''apparent'' polarization were also examined. © *2004 American Institute of Physics.* [DOI: 10.1063/1.1759078]

I. INTRODUCTION

The polarization behaviors of ferroelectric films have attracted great research interest for many years because of applications in a variety of devices such as ferroelectric memories, infrared pyroelectric sensors, and microelectromechanical systems. In the past, it has been demonstrated that the hysteresis loop of ferroelectric films, usually measured by the Sawyer-Tower circuit,[1] can exhibit inflation (or deformations). This can be originated from the resistive loss of the material.[2,3] This effect can normally be neglected if the measuring frequency is sufficiently high. However, some ferroelectrics may possess high electrical conductivity which enhances the effect at higher frequency range. This ''leaky'' character can originate from doping, processing conditions, temperature, etc.[4–6] In the literature, some modified Sawyer-Tower circuit arrangements do exist to compensate for the resistive loss effect,[7,8] and both experimental and theoretical investigations of the ferroelectric hysteresis behavior with conduction phenomena have been studied for many years.[3,9–12] Some sophisticated modeling approaches have also been suggested which were claimed to faithfully simulate the polarization and conduction behavior. However, difficult numerical computation schemes must invariably be employed to get predictions of the apparent polarization. In contrast, we aim in this paper to obtain simple explicit expressions for the most important characteristics of polarization behavior under ac conduction. The end results will be useful as a quick reference in analyzing experimental data.

In addition, many hysteresis loop measured using the Sawyer-Tower circuit also exhibit voltage offset along the horizontal[13,14] and vertical[15,16] axes in thin film ferroelectrics. This may be due to asymmetric characters of the film on substrate: one side of the film is next to the substrate, the other exposed to air or vacuum. This difference in contact causes the polarization and other properties to exhibit directional characteristics (hence asymmetry). Asymmetric electrodes and different thermal treatments on the top and bottom interfaces also lead to an asymmetric hysteresis loop. There have been some theoretical studies on the horizontal (electric field) shift of hysteresis loops,[17–21] but the studies of vertical (electric displacement) shift are still scarce in the literature. Zheng *et al.* measured the asymmetric current–voltage characteristics of lead zirconate titanate (PZT) films as well as the vertical offset of hysteresis loops.[15,22,23] They suggested that the barrier heights or contact types at the two electrode-film interfaces were different, which led to the asymmetric leakage current and was the origin of the polarization offset. They also developed a model for describing the vertical offset of the hysteresis loop, but they did not consider the coupled electric conduction, dielectric and ferroelectric properties. The phenomena of asymmetric leakage current have also been observed in other thin film materials,[16,24,25] and the origin of asymmetric leakage current in heterostructures have been discussed in literature.[26–28] On the other hand, the anomalous vertical offset of hysteresis loops observed in graded ferroelectric films (e.g., temperature or compositionally graded) was also suggested to be an effect of asymmetrical leakage current.[29] Recently, Bouregba *et al.* demonstrated this idea by setting diodes and resistors in parallel with a nongraded structure.[30] Without considering the role of ferroelectric properties (in their theoretical analysis, the ferroelectric sample is treated as a series connection of a linear resistor and a diode), they obtained an expression for the dynamic behavior of polarization offset. All in all, previous analytical models treated the ferroelectric sample at most as a linear dielectric to study the polarization offset.

To gain a deeper understanding of the offset mechanism under investigation, it is desirable to use a simple but rigorous analytical model to investigate the behavior of the system in broad terms. However, it is not easy to develop very detailed analytical models since the ferroelectric hysteresis loop is highly nonlinear. In this paper, we propose to use a parallelogramlike hysteresis loop to model the ferroelectric properties of the sample. A similar approach was also adopted by Kanashima and Okuyama to study the $C-V$ characteristics of the metal-ferroelectric-insulator-silicon structure[31] and by Hauke *et al.* who studied the poling behavior of ferroelectric 1–3 composites.[32] Assuming the ferroelectric with finite symmetric or asymmetric conductivities is placed in a Sawyer-Tower circuit, we attempt to derive exact equations to study the inflated and offset polarization loops. When solving the model equations, different regions of the parallelogramlike hysteresis loop have to be separately considered and the applied field is taken as triangular wave. In this case, exact solution in different regions can be obtained. The results are then combined to obtain an expression characterizing the dynamic behavior of the polarization loop. Explicit formulas for the apparent remanent polarizations in a number of different conductivities regions have been obtained. Summing up, our derivations are free of approximations, and the end results, which have incorporated the coupled electric, dielectric, and ferroelectric properties, are simple and tractable. The effects of the applied ac field, electric, dielectric, and ferroelectric properties on the various important phenomena will be systemically examined. Discussions on the experimental data of Miller *et al.*[3] and Bouregba *et al.*[30] will also be made.

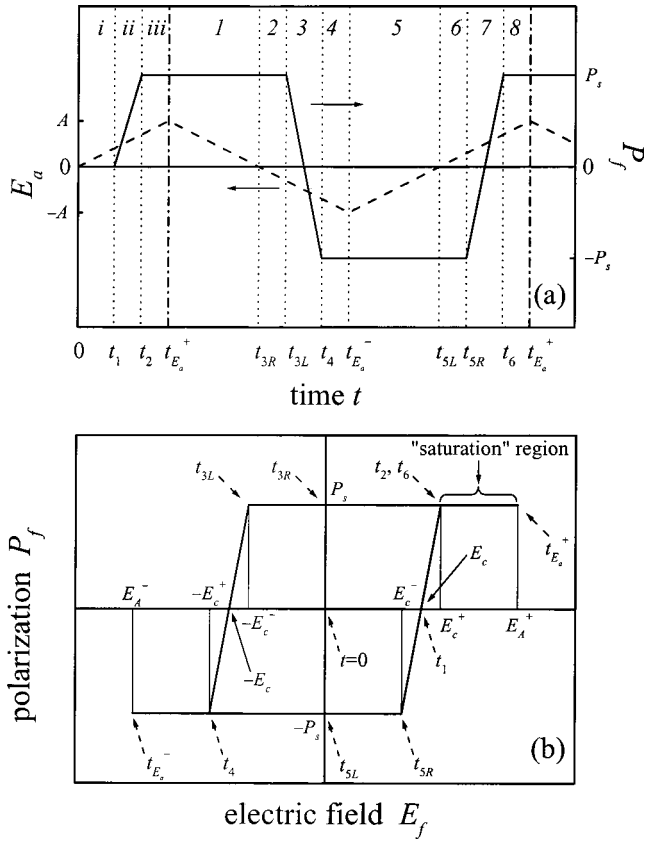

FIG. 1. (a) The variation of the applied field E_a (dashed line) and polarization P_f (solid line) with time. Regions $i-iii$ are the initial regions and regions *1–8* are the looping regions. (b) A multilinear, parallelogramlike P_f-E_f hysteresis loop.

II. FERROELECTRIC-DIELECTRIC LAYERED MODEL

Our model assumes that the hysteresis loop is measured by a Sawyer-Tower circuit. The Sawyer-Tower measurement circuit is merely a capacitor divider where the ferroelectric sample is in series with a standard reference capacitor. The electric displacement of the sample is calculated from the voltage measured across the reference capacitor. Usually two assumptions are made in the measurement: electric displacements across the sample and reference capacitor are identical and the capacitance of the reference capacitor is much larger than that of the sample. This configuration for measuring the D-E loop of a ferroelectric film can be modeled by a double-layer structure with the capacitor being a nonferroelectric (dielectric) layer. The constitutive equations are

$$D_f = \epsilon_f E_f + P_f, \qquad D_d = \epsilon_d E_d, \tag{1}$$

where D is electric displacement, P is polarization, ϵ is permittivity, and E is electric field. Subscripts f and d denote the ferroelectric film and reference capacitor, respectively.

Assuming for convenience that the sample and reference capacitor have identical thickness, the applied electric field on the system (E_a) is given by

$$E_a = (E_f + E_d)/2. \tag{2}$$

We also assume the sample material supports a finite conductivity so that charges may flow, but the standard capacitor is a perfect insulator. Thus, the boundary conditions require

$$\sigma_f^{\pm} E_f + \frac{\partial D_f}{\partial t} = \frac{\partial D_d}{\partial t}, \tag{3}$$

where σ is electrical conductivity. The superscript "$\pm$" denotes σ_f may take different values for $E_f > 0$ (represented by "$+$") and $E_f < 0$ (represented by "$-$"). This usage is consistent with the notation adopted by Zheng *et al.*[15] and Bouregba *et al.*[30] Using Eqs. (1)–(3), we obtain, after some manipulation,

$$(1+x+y)\frac{\partial E_f}{\partial t} + \frac{E_f}{\tau_f^{\pm}} = 2x\frac{\partial E_a}{\partial t}, \tag{4}$$

where $x = \epsilon_d/\epsilon_f$, $y = (\partial P_f/\partial E_f)/\epsilon_f$, and $\tau_f^{\pm} = \epsilon_f/\sigma_f^{\pm}$. For a given external ac field E_a, we may obtain E_f as a function of time t when the P-E relation for the sample is known. Then the D-E loop of the sample (as measured by a Sawyer-Tower circuit) can be obtained from the electric field across the standard capacitor and the electric field across the sample. In this work, the applied electric field is a triangular wave [Fig. 1(a)] and the hysteresis loop is taken as a parallelogram [Fig. 1(b)]. In Fig. 1, three initial regions (regions $i-iii$) and eight looping regions (regions *1–8*) have been located. It is seen

that $\partial P_f/\partial E_f$ becomes a constant ($\equiv m_f$) for $t_{3L} \leqslant t \leqslant t_4$ or $t_{5R} \leqslant t \leqslant t_6$, and becomes zero elsewhere. The solutions of solving Eq. (4) for each region are

Region i: $$E_f(t \leqslant t_1) = 2m_a x \tau_f^+ (1 - e^{-t/(1+x)\tau_f^+}), \quad (5)$$

Region ii: $$E_f(t_1 \leqslant t \leqslant t_2) = 2m_a x \tau_f^+ + (E_c - 2m_a x \tau_f^+) \times e^{(-t+t_1)/(1+x+y)\tau_f^+}, \quad (6)$$

Region iii: $$E_f(t_2 \leqslant t \leqslant t_{Ea}^+) = 2m_a x \tau_f^+ + (E_c^+ - 2m_a x \tau_f^+) \times e^{(-t+t_2)/(1+x)\tau_f^+}, \quad (7)$$

Region 1: $$E_f(t_{Ea}^+ \leqslant t \leqslant t_{3R}) = -2m_a x \tau_f^+ + (E_A^+ + 2m_a x \tau_f^+) \times e^{(-t+t_{Ea}^+)/(1+x)\tau_f^+}, \quad (8)$$

Region 2: $$E_f(t_{3R} \leqslant t \leqslant t_{3L}) = -2m_a x \tau_f^- (1 - e^{(-t+t_{3R})/(1+x)\tau_f^-}), \quad (9)$$

Region 3: $$E_f(t_{3L} \leqslant t \leqslant t_4) = -2m_a x \tau_f^- - (E_c^- - 2m_a x \tau_f^-) e^{(-t+t_{3L})/(1+x+y)\tau_f^-}, \quad (10)$$

Region 4: $$E_f(t_4 \leqslant t \leqslant t_{Ea}^-) = -2m_a x \tau_f^- - (E_c^+ - 2m_a x \tau_f^-) \times e^{(-t+t_4)/(1+x)\tau_f^-}, \quad (11)$$

Region 5: $$E_f(t_{Ea}^- \leqslant t \leqslant t_{5L}) = 2m_a x \tau_f^- + (E_A^- - 2m_a x \tau_f^-) \times e^{(-t+t_{Ea}^-)/(1+x)\tau_f^-}, \quad (12)$$

Region 6: $$E_f(t_{5L} \leqslant t \leqslant t_{5R}) = 2m_a x \tau_f^+ (1 - e^{(-t+t_{5L})/(1+x)\tau_f^+}), \quad (13)$$

Region 7: $$E_f(t_{5R} \leqslant t \leqslant t_6) = 2m_a x \tau_f^+ + (E_c^- - 2m_a x \tau_f^+) \times e^{(-t+t_{5R})/(1+x+y)\tau_f^+}, \quad (14)$$

Region 8: $$E_f(t_6 \leqslant t \leqslant t_{Ea}^+) = 2m_a x \tau_f^+ + (E_c^+ - 2m_a x \tau_f^+) \times e^{(-t+t_6)/(1+x)\tau_f^+}, \quad (15)$$

where

$$t_1 = -(1+x)\tau_f^+ \ln\left(1 - \frac{E_c}{2m_a x \tau_f^+}\right), \quad (16)$$

$$t_2 = t_1 - (1+x+y)\tau_f^+ \ln\left(\frac{E_c^+ - 2m_a x \tau_f^+}{E_c - 2m_a x \tau_f^+}\right), \quad (17)$$

$$t_{3R} = t_{Ea}^+ + (1+x)\tau_f^+ \ln\left(1 + \frac{E_A^+}{2m_a x \tau_f^+}\right), \quad (18)$$

$$t_{3L} = t_{3R} - (1+x)\tau_f^- \ln\left(1 - \frac{E_c^-}{2m_a x \tau_f^-}\right), \quad (19)$$

$$t_4 = t_{3L} - (1+x+y)\tau_f^- \ln\left(\frac{E_c^+ - 2m_a x \tau_f^-}{E_c^- - 2m_a x \tau_f^-}\right), \quad (20)$$

$$t_{5L} = t_{Ea}^- + (1+x)\tau_f^- \ln\left(1 - \frac{E_A^-}{2m_a x \tau_f^-}\right), \quad (21)$$

$$t_{5R} = t_{5L} - (1+x)\tau_f^+ \ln\left(1 - \frac{E_c^-}{2m_a x \tau_f^+}\right), \quad (22)$$

$$t_6 = t_{5R} - (1+x+y)\tau_f^+ \ln\left(\frac{E_c^+ - 2m_a x \tau_f^+}{E_c^- - 2m_a x \tau_f^+}\right), \quad (23)$$

and $m_a = 4A/T$, $E_c^+ = E_c + P_s/m_f$, $E_c^- = E_c - P_s/m_f$. Symbols A and T represent the amplitude and period of the applied electric field. E_A^+ and E_A^- are the electric field across the sample when $E_a = A$ and $-A$, respectively ($t = t_{Ea}^+$ and t_{Ea}^-, respectively). For the first quarter period E_f can be calculated by Eqs. (5)–(7), and for the subsequent period by Eqs. (8)–(15). More periods may be calculated repeatedly by applying Eqs. (8)–(15) with t_{Ea}^+ and E_A^+ updated recursively. The ''measured'' electric displacement of the sample may then be calculated by $D = D_d = \epsilon_d(2E_a - E_f)$.

From Eqs. (7), (16), and (17), E_A^+ at $t = T/4$ is obtained as

$$E_A^+(T/4) = 2m_a x \tau_f^+ \times \left\{1 - \left(\frac{E_c^+ - 2m_a x \tau_f^+}{E_c - 2m_a x \tau_f^+}\right)^{-y/(1+x)} e^{-T/4(1+x)\tau_f^+}\right\}. \quad (24)$$

For subsequent cycles, a recursive function for describing the periodic changes of E_A^+ may be obtained by first considering $t = t_{Ea}^+$ in Eq. (15) with the resultant equation giving $E_A^+(t+T)$. Since we are going to derive an equation relating $E_A^+(t+T)$ and $E_A^+(t)$, we eliminated all t's to obtain $E_A^+(t)$ by substituting Eqs. (18)–(23) with E_A^+ in Eq. (18) replaced by $E_A^+(t)$. E_A^- in Eq. (21) is eliminated by making use Eq. (11) with $E_A^- = E_f(t = t_{Ea}^+ - T/2)$. Thus, the result is

$$E_A^+(t+T) = 2m_a x \tau_f^+ \left\{1 - \alpha^+ \left[2 - \alpha^- \left(1 + \frac{E_A^+(t)}{2m_a x \tau_f^+}\right)^z \times e^{-T/2(1+x)\tau_f^-}\right]^{1/2} e^{-T/2(1+x)\tau_f^+}\right\}, \quad (25)$$

where

$$\alpha^\pm = \left(\frac{E_c^+ - 2m_a x \tau_f^\pm}{E_c^- - 2m_a x \tau_f^\pm}\right)^{-y/(1+x)} \quad (26)$$

and $z=\sigma_f^-/\sigma_f^+$. In general, it is not easy to obtain exact analytical results from Eq. (25). However, by iterating Eq. (25) for the desired number of measuring periods, the dynamics of the remanent polarization in the hysteresis loop as measured by the Sawyer-Tower arrangement may be calculated by

$$P_r^+=\frac{m_a\epsilon_d}{2}\left[T-4(1+x)\tau_f^+\ln\left(\frac{1+E_A^+}{2m_ax\tau_f^+}\right)\right], \tag{27}$$

$$P_r^-=-\frac{m_a\epsilon_d}{2}\left[T-4(1+x)\tau_f^-\ln\left(\frac{1+E_A^-}{2m_ax\tau_f^-}\right)\right], \tag{28}$$

where

$$E_A^-=-2m_ax\tau_f^-\left\{1-(\alpha^+)^{-z}\left(1-\frac{E_A^+}{2m_ax\tau_f^+}\right)^z\times e^{T/2(1+x)\tau_f^-}\right\}. \tag{29}$$

In Eqs. (27) and (28), P_r^+ and P_r^- refer to the measured polarization at $t=t_{3L}$ and t_{5R}, respectively. Thus, the polarization offset can be calculated by $D_{off}=(P_r^++P_r^-)/2$.

When $z=1$ which corresponds to symmetric conductivity $\sigma_f^+=\sigma_f^-=\sigma_f$ and thus $\tau_f^+=\tau_f^-=\tau_f$ and $\alpha^+=\alpha^-=\alpha$, Eq. (25) can be exactly solved. P_r^+ and P_r^- [Eqs. (27) and (28)] can then be calculated via $E_A^+|_{z=1}$ and $E_A^-|_{z=1}$:

$$E_A^+|_{z=1}=\left(E_A^+(T/4)|_{z=1}+2m_ax\tau_f\frac{\alpha-e^{T/2(1+x)\tau_f}}{\alpha+e^{T/2(1+x)\tau_f}}\right)\times(\alpha e^{-T/2(1+x)\tau_f})^{2j}-2m_ax\tau_f\frac{\alpha-e^{T/2(1+x)\tau_f}}{\alpha+e^{T/2(1+x)\tau_f}}, \tag{30}$$

$$E_A^-|_{z=1}=\frac{1}{\alpha}\{E_A^+|_{z=1}+2m_ax\tau_f(\alpha-e^{T/2(1+x)\tau_f})\}, \tag{31}$$

where $j=0,1,2,...,k-1$ and k is the desired number of measuring periods.

Concerning the saturated values of P_r^+, P_r^-, and D_{off}, they may also be obtained by solving Eq. (25) with $E_A^+(t+T)=E_A^+(t)$. The results for $z=2$ (i.e., asymmetric conduction), after substituting into Eqs. (27) and (28), are

$$P_r^+(\text{sat})|_{z=2}=\frac{m_a\epsilon_d}{2}\left[T-4(1+x)\tau_f^+\times\ln\left(\frac{2\gamma^2-\alpha^+\sqrt{2\gamma(\gamma^2-2\alpha^-\gamma+\alpha^{+2}\alpha^-)}}{\gamma^2+\alpha^{+2}\alpha^-}\right)\right], \tag{32}$$

$$P_r^-(\text{sat})|_{z=2}=\frac{-m_a\epsilon_d}{2}\left[T-8(1+x)\tau_f^-\times\ln\left(\frac{2\alpha^+\alpha^-\gamma^{1/2}-\sqrt{2\gamma(\gamma^2-2\alpha^-\gamma+\alpha^{+2}\alpha^-)}}{\gamma^2+\alpha^{+2}\alpha^-}\right)\right], \tag{33}$$

where $\gamma\equiv\exp\{T/[2(1+x)\tau_f^-]\}$. When $z=1$ (i.e., symmetric conduction), we obtain

$$P_r^+(\text{sat})|_{z=1}=\frac{m_a\epsilon_d}{2}\left[T-4(1+x)\tau_f\ln\left(\frac{2}{1+\alpha e^{-T/2(1+z)\tau_f}}\right)\right], \tag{34}$$

$$P_r^-(\text{sat})|_{z=1}=-P_r^+(\text{sat})|_{z=1}. \tag{35}$$

Note that the polarization offset $[D_{off}=(P_r^++P_r^-)/2]$ is zero, and $P_r^+(\text{sat})|_{z=1}$ and $P_r^-(\text{sat})|_{z=1}$ approach P_s and $-P_s$ respectively, when σ_f (in α and τ_f) tends to zero. On the other hand, under the limiting case that x tends to infinity (an ideal reference capacitor), Eqs. (34) and (35) become

$$P_r^+(\text{sat})|_{x\to\infty}^{z=1}=P_s+AT\sigma_f/4, \tag{36}$$

$$P_r^-(\text{sat})|_{x\to\infty}^{z=1}=-P_s-AT\sigma_f/4, \tag{37}$$

which shows the inflated remanent polarization of the measured loop is proportional to the conductivity of the sample.

In summary, Eq. (25) describes a general dynamic behavior for all z's, and Eq. (30) may be used for symmetric conduction. Eqs. (32) and (33) describe the saturated remanent polarization values for asymmetric conduction when $z=2$ and Eqs. (34) and (35) for symmetric conduction ($z=1$). However, if one wants to obtain saturated values of P_r^+, P_r^-, and D_{off} for more general asymmetric conductivity of the ferroelectric sample (e.g., $z>2$), numerical solution of Eq. (25) may be obtained by setting $E_A^+(t+T)=E_A^+(t)$.

III. RESULTS AND DISCUSSION

In this section, theoretical predictions based on the foregoing expressions with symmetric and asymmetric conductivities are separately investigated. Table I shows all adopted values for the applied field, as well as the properties of the ferroelectric sample and reference capacitor, for our predictions in each figure.

A. Polarization behavior in ferroelectrics with finite conductivity

We will first concentrate on the polarization behavior of ferroelectric samples with symmetric conductivity (i.e., $z=1$). Actually, the hysteresis loop measured by a Sawyer-Tower circuit for an ideal ferroelectric sample ($\sigma=0$) should be free from distortions or deformations. In reality, all ferroelectrics possess some finite conductivity. This allows charge transport and accumulation, which results in some phase shift between the D and E fields which displaces the mea-

TABLE I. The magnitude and period of applied field, and the properties of the sample and reference capacitor used in the calculations.

Figure	A (V μm^{-1})	T (s)	m_f (10^{-8} Fm^{-1})	P (μC cm^{-2})	E_c (V μm^{-1})	ϵ_f/ϵ_0	σ_f^+ ($10^{-11}\,\Omega^{-1}$ cm^{-1})	σ_f^- ($10^{-11}\,\Omega^{-1}$ cm^{-1})	$x \equiv \epsilon_d/\epsilon_f$
2	10	Varied	30	20	5	500	1	1	100
3	10	100	30	20	5	500	1	1	Varied
4	10	Varied	30	20	5	500	1	1	Varied
5	Varied	0.02	30	20	5	500	Varied	Varied	100
6	10	100	30	20	5	500	0.5	1	Varied
7	Varied	0.02	30	20	5	500	10^{-4} to 1	Varied	100
8	10	50	30	20	5	Varied	10^{-4} to 1	Varied	100
9	10	Varied	30	20	5	500	1	2	Varied
10	10	Varied	30	Varied	5	500	1	2	100
11	50	Varied	30	20	Varied	500	1	2	100

sured hysteresis loop from the true loop. Usually, this resistive effect is only significant at low measurement frequency. However, for ferroelectrics possessing higher conductivity, we ought to include such consideration at higher frequency. Figure 2 shows the variation of the D_d-E_f hysteresis loop (i.e., the hysteresis loop of the sample measured by a Sawyer-Tower circuit) with respect to different values of the period T of the applied field. For a short enough period (higher frequency), the shape of the hysteresis loop is almost the same as the original parallelogramlike loop. However, the hysteresis loop inflates as the adopted period increases (reduced frequency). On the other hand, if one fixes the measurement frequency (say 10 Hz) but increases the sample conductivity, similar inflated loops are observed. This means both low frequency and high conductivity can significantly distort hysteresis loops. The results also show that excessive increasing of period distorts the "saturation" region of the loops, from basically a pair of lines slightly inclined to the E_f axis to a ">" or "<" shape, and thus the magnitude of the "apparent" remanent polarization (i.e., P_r^+ and P_r^-) increases in an obvious way (details will be discussed in connection with Fig. 4). These characteristics were also demonstrated by Miller *et al.*[3] They measured the hysteresis loops of ferroelectric capacitors and found inflation with decreasing frequency; the main features of the distorted loop shapes are also in good agreement with our results. On the other hand, the variation in the apparent coercive field E_c^{app} of the sample is small for periods $T<10$ s (in this calculation, E_c^{app} changes at most by 13% of E_c). For longer ac periods ($T>10$ s), the coercive field increases rapidly until saturation is achieved. In the literature, the experimental results for the effect of measurement frequency on E_c^{app} had also been reported.[3] Comparing with Ref. 3, all key features in the behavior of E_c^{app} are qualitatively reproduced by our model.

In Fig. 3, the dynamic behavior of P_r^+ and P_r^- with different values of x at low frequency ($T=100$ s) are calculated [Eqs. (30) and (31) via Eqs. (27) and (28)]. The results show that, at the end of the first cycle, the magnitudes of P_r^+ and P_r^- are substantially greater than P_s for $x=50-1000$, and $|P_r^+|$ is also greater than $|P_r^-|$ (i.e., an initial net polarization offset). Thus the hysteresis loop of the sample is shifted up by $D_{off}=(P_r^+ + P_r^-)/2$. As more ac cycles are measured, the magnitudes of P_r^+ and P_r^- decrease exponentially [see Eq. (30)] and they converge to $P_r^+(\text{sat})$ and $P_r^-(\text{sat})$ [Eqs. (34) and (35)], respectively. In other words, the vertical shifts of the loop decreases and reduces to zero for a sufficiently large number of cycles. On the other hand, an initially larger up-shift of the hysteresis loop and a slower relaxation of polarization offset are observed for a larger x.

Concerning the polarization P_r^+ at steady state, the variation of $P_r^+(\text{sat})$ with respect to the period T of the applied field with different values of x is illustrated in Fig. 4. The figure shows that all profiles of $P_r^+(\text{sat})$ versus T con-

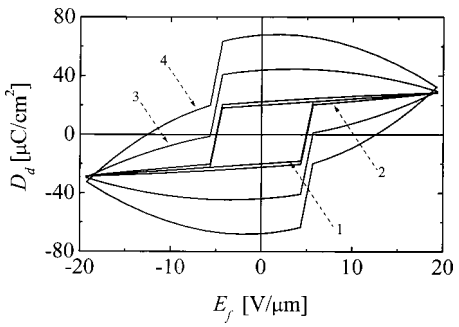

FIG. 2. The variation of the D_d-E_f hysteresis loop corresponding to different values of the period T of the applied field. The period T is 0.1 s, 10 s, 100 s, and 200 s for the loops 1, 2, 3, and 4, respectively.

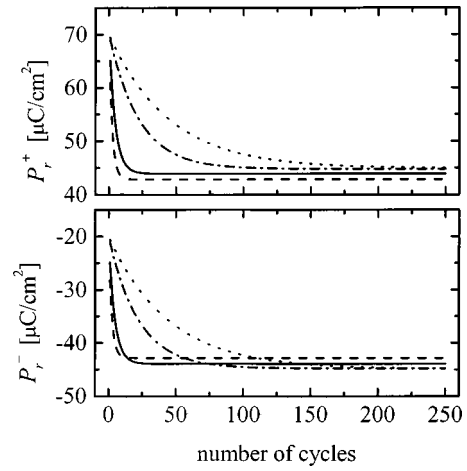

FIG. 3. The variation of the polarization P_r^+ and P_r^- with the number of cycles. The dashed, solid, dash-dotted, and dotted lines denote $x=50$, $x=100$, $x=500$, and $x=1000$, respectively.

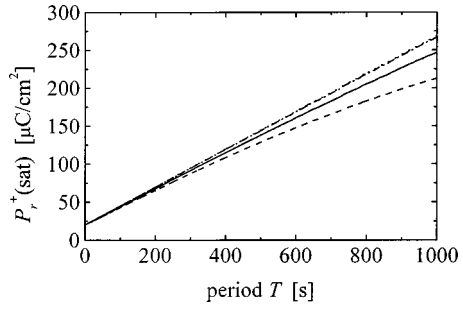

FIG. 4. The variation of the polarization $P_r^+(\text{sat})$ with the period T of the applied field. The dashed, solid, dash-dotted, and dotted lines denote $x=50$, $x=100$, $x=500$, and $x=1000$, respectively. The latter two curves are almost overlapping.

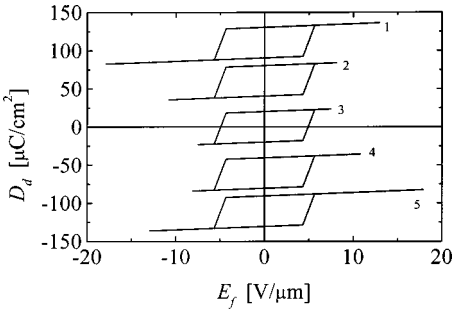

FIG. 5. The variation of the steady state D_d-E_f hysteresis loop with the amplitude A of the applied field. The amplitude A is 8 V/μm for loops 1 and 5. Whilst, the amplitude A is 4 V/μm for loops 2, 3, and 4. $z=2$ for loops 1 and 2, $z=1$ for loop 3, and $z=0.5$ for loops 4 and 5.

verge to the same limiting value, which is P_s, for small T. Increasing period T or x, $P_r^+(\text{sat})$ strictly increases. For a sufficiently large x, the profile of $P_r^+(\text{sat})$ versus T tends to a straight line, which is also described by Eq. (36). With regard to the work of Miller *et al.* $P_r^+(\text{sat})$ was also shown to be larger than the ''true value'' of remanent polarization and $P_r^+(\text{sat})$ increased with decreasing frequency.[3] In view of these features and those discussed in relation to Fig. 2, it seems that our model have captured the most important characters of a hysteresis loop measured at different frequencies for different durations. Since x promotes the value of $P_r^+(\text{sat})$ and the capacitance of the reference capacitor is directly proportional to $\epsilon_d = x\,\epsilon_f$, a high capacity of the reference capacitor would raise the magnitudes of P_r^+ and P_r^-. In the above, our investigations are thought to be valid for an experimental system with a high impedance oscilloscope, which is generally essential. Otherwise, the response predicted in Fig. 4 may no longer apply. We have chosen to neglect the consideration of oscilloscope impedance because this is considered a secondary effect from external components. Moreover, the analytic results will become dramatically more complicated.

B. Polarization offsets in ferroelectrics with asymmetric conductivities

In this section, we will discuss the polarization behavior of the ferroelectric sample with asymmetric conductivities (i.e., $z\neq 1$). In the past, some experimental results have demonstrated that the measured hysteresis loop may drift vertically and a possible origin is the asymmetric conductivity.[15,16,22–25] On the other hand, similar drift phenomena also exist in compositionally graded ferroelectrics. However, the drift magnitude might be surprisingly large and was reported to be an order larger than the spontaneous polarization.[33–35] Although our model assumes a single ferroelectric sample, our analysis is thought to be roughly valid for a graded ferroelectric, which is a multilayered composite. A composite possesses effective dielectric and ferroelectric properties, and we imagine this ''effective'' sample is placed in the Sawyer-Tower circuit. Figure 5 shows the variation of the steady state D_d-E_f hysteresis loop corresponding to different values of the amplitude A of the applied field. For reference, the figure also shows a hysteresis loop (loop 3) with symmetric conductivity ($z=1$), i.e., no polarization offset observed. For $z\neq 1$, the D_d-E_f loop shifts either up ($z=0.5<1$ for loop 2) or down ($z=2>1$ for loop 4). It is obvious that the magnitude of D_{off} is identical for loop 2 and loop 4, which have adopted reciprocal z values. Also, the vertical shift increases as the amplitude A increases (cf. loops 2 and 4 with loops 1 and 5). Interestingly, the shapes of all loops (1–5) are almost the same. In other words, it seems that the ''central region'' of the D_d-E_f loops (loops 1, 2, 4, and 5) only translates vertically by D_{off} from the origin.

In Fig. 6, the dynamic profiles of D_{off} with different values of x are illustrated. Our modeled dynamic behavior showing an exponential increasing/decreasing phenomenon agrees with the experimental results for graded ferroelectrics of Brazier *et al.*,[36] as well as the analysis by Bouregba *et al.*[30] At the first cycle, $D_{off}\neq 0$. Thus, the D-E loop of the sample is initially shifted by D_{off}. As the number of cycle increases, the magnitudes of D_{off} gradually increase and converge to the limiting values [calculated by Eqs. (32) and (33)]. In other words, the vertical shift of the loop increases and converges to a limiting value for a sufficiently large cycle number. This phenomenon is different from the case of symmetric conduction ($z=1$), i.e., $D_{off}(\text{sat})\neq 0$ for $z\neq 1$ but $D_{off}(\text{sat})=0$ for $z=1$. When the magnitude of x increases, the magnitude of $D_{off}(\text{sat})$ increases. Note that the capacitance of the reference capacitor is directly proportional to $\epsilon_d = x\,\epsilon_f$. Therefore, high capacitance should promote the magnitude of $D_{off}(\text{sat})$. This agrees with the analysis reported by Bouregba *et al.*[30]

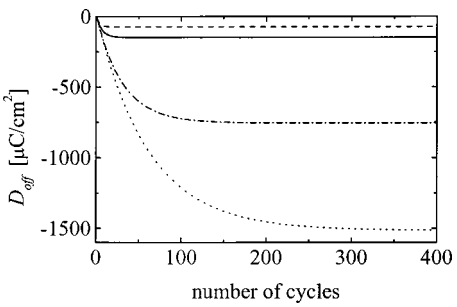

FIG. 6. The variation of D_{off} with the number of cycles. The dashed, solid, dash-dotted, and dotted lines denote $x=50$, $x=100$, $x=500$, and $x=1000$, respectively.

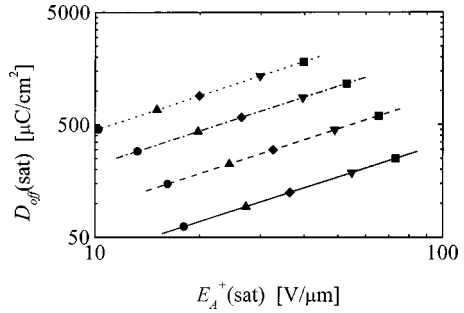

FIG. 7. The variation of $D_{off}(\text{sat})$ with the magnitude $E_A^+(\text{sat})$ of the electric field across sample. The symbols ●, ▲, ◆, ▼, and ■ denote the corresponding amplitude A of the applied field: 10 V/μm, 15 V/μm, 20 V/μm, 30 V/μm, and 40 V/μm, respectively. The solid, dashed, dash-dotted, and dotted lines denote the electrical conductivity ratio $z=0.75$, 0.5, 0.25, and 0.1, respectively.

The effects of electric and dielectric properties of the sample on $D_{off}(\text{sat})$ are demonstrated in Figs. 7 and 8, respectively. In Fig. 7, the variation of $D_{off}(\text{sat})$ with respect to $E_A^+(\text{sat})$ (the electric field across the sample at steady state when $E_a=A$) for different values of the conductivity ratio z is shown. For a fixed z, the results show that the magnitude of $D_{off}(\text{sat})$ is directly proportional to $E_A^+(\text{sat})$. In addition, the profiles of $D_{off}(\text{sat})$ with different values of z are exactly parallel to each other with $D_{off}(\text{sat})$ increasing as higher asymmetry in z is introduced. However, in the literature, the relationship between $D_{off}(\text{sat})$ and $E_A^+(\text{sat})$ generally obeys a power law,[30,34,35] i.e., $D_{off}(\text{sat}) \propto E_A^+(\text{sat})^n$, $2 \lesssim n \lesssim 5$, which differ from the present results. The possible reason is that, in our calculation, σ_f^+ and σ_f^- are assumed to be constants independent of $E_A^+(\text{sat})$. However, for large applied fields, the relationship between current and electric field may become highly nonlinear, and the conductivity may increase with the field strength.[6] Many previous works had reported such phenomena and the difference between σ_f^+ and σ_f^- (i.e., asymmetry) may also increase with the field strength.[22,30] If our adopted ohmic conduction is replaced by other mechanisms such that asymmetry in conductivity increases with field, then n in the power law could be made larger than 1. However, exact analytical modeling may not be possible and numerical simulations should be employed.

In Fig. 8, the variation of $D_{off}(\text{sat})$ with respect to the permittivity ϵ_f of the sample with different values of the conductivity ratio z is illustrated. For a fixed z, $D_{off}(\text{sat})$ increases linearly with ϵ_f. As z is far away from 1 (more asymmetric), the slope of the profile of $D_{off}(\text{sat})$ increases. Note that in Figs. 7 and 8, the trends of each line are almost the same for different values of z. In addition, for the same value of z (fixed asymmetry), overlapping predictions are shown for a wide range of σ_f^+ (Table I). It demonstrates that the polarization offsets are mainly dictated by the asymmetry of conductivities, rather than their magnitudes. Many experimental results on graded ferroelectrics reported some very large polarization offsets. Even though their films may originally possess very low conductivities, such phenomenon can still originate from a large asymmetry in the ''effective'' conductivity of the sample, due to, e.g., internal stress and lattice mismatch across the composition gradient. Since our model assumes symmetric properties other than conductivity, it is expected that the modeled behavior for a chosen z will almost be identical (albeit differing by a sign) to that for reciprocal z. In Sec. II, we have derived explicit formulas for the predictions of $P_r^+(\text{sat})$ and $P_r^-(\text{sat})$ at $z=2$ [Eqs. (32) and (33)]. We have verified that the predictions of these formulas is the ''reverse'' of those given in Figs. 7 and 8 for $z=0.5$.

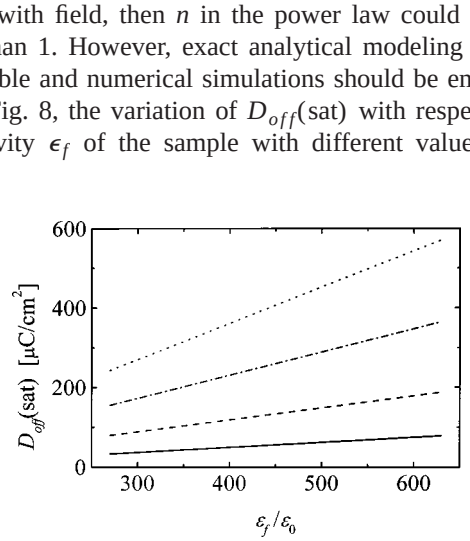

FIG. 8. The variation of $D_{off}(\text{sat})$ with the dielectric constant ϵ_f/ϵ_0 of the sample. The solid, dashed, dash-dotted, and dotted lines denote the electrical conductivity ratio $z=0.75$, 0.5, 0.25, and 0.1, respectively.

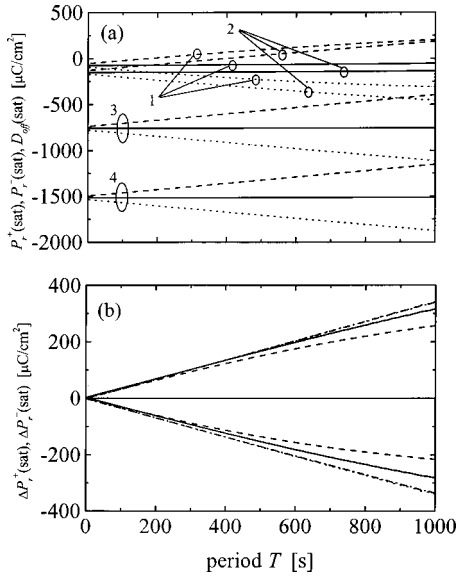

FIG. 9. (a) The variation of $P_r^+(\text{sat})$, $P_r^-(\text{sat})$, and $D_{off}(\text{sat})$ with the period T of the applied field. The dashed, dotted, and solid lines denote $P_r^+(\text{sat})$, $P_r^-(\text{sat})$, and $D_{off}(\text{sat})$, respectively. The lines marked with 1, 2, 3, and 4 denote $x=50$, $x=100$, $x=500$, and $x=1000$, respectively. (b) The variation of $\Delta P_r^+(\text{sat})$ and $\Delta P_r^-(\text{sat})$ with the period T of the applied field. The dashed, solid, dash-dotted, and dotted lines denote $x=50$, $x=100$, $x=500$, and $x=1000$, respectively.

Effects of the period of the applied field and the ferroelectric properties (including P_s and E_c) of the sample on $D_{off}(\text{sat})$ can also be described by Eqs. (32) and (33). Recalling that these formulas assume $z=2$, such effects [$D_{off}(\text{sat})$ versus T, P_s, and E_c] are demonstrated in Figs. 9, 10, and 11. Figure 9(a) shows the variation of $P_r^+(\text{sat})$, $P_r^-(\text{sat})$, and $D_{off}(\text{sat})$ with respect to the period T for different values of x. Clearly, the magnitudes of $P_r^+(\text{sat})$ and $P_r^-(\text{sat})$ are not identical, thus $D_{off}(\text{sat})$ is nonzero for $z \neq 1$. For a fixed x, the magnitudes of $P_r^+(\text{sat})$ and $P_r^-(\text{sat})$

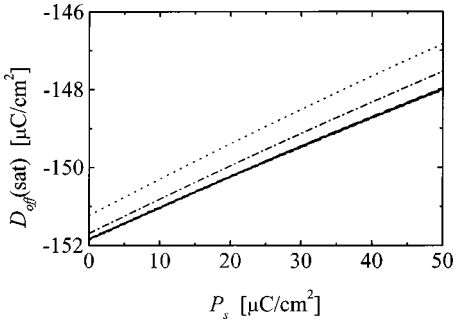

FIG. 10. The variation of D_{off}(sat) with P_s of the sample. The solid, dashed, dash-dotted, and dotted lines denote the period $T=0.1$ s, 10 s, 100 s, and 200 s, respectively.

increase with the period T, and D_{off}(sat) almost does not vary with T. This demonstrates the measuring frequency does not affect the effect of polarization offset significantly, owing to asymmetric conduction. However, as T increases (reduced frequency) the resistive effect comes into play, which inflates ferroelectric loops. Consequently, a vertically shifted inflated hysteresis loop will be observed. Figure 9(b) shows the variation of $\Delta P_r^+(\text{sat})[\equiv P_r^+(\text{sat})-P_r^+(T/2)]$ and $\Delta P_r^-(\text{sat})[\equiv P_r^-(\text{sat})-P_r^-(T)]$ with respect to the period T for different values of x. For a sufficiently large x, the profiles of $\Delta P_r^+(\text{sat})$ and $\Delta P_r^-(\text{sat})$ versus T tend to straight lines, which can also be traced from Eqs. (32) and (33), respectively. Overall, the D_d-E_f loops inflate as T increases and these effects are the same as the case for $z=1$ (Fig. 4). Moreover, a high capacity of the reference capacitor dramatically promotes polarization offsets. In Fig. 10, the variation of the D_{off}(sat) with respect to P_s is shown with different periods T of the applied field. When either the period T or P_s decreases, the magnitude of D_{off}(sat) increases [described by Eqs. (32) and (33) via $D_{off}=(P_r^+ + P_r^-)/2$], but the effect is not as pronounced as that from field amplitude, asymmetry in conductivities, permittivity, and the capacity of reference capacitor (see Figs. 7–9). In addition, the behavior of the D_{off}(sat) versus P_s is almost linear. The slope of the profile of the $|D_{off}(\text{sat})|$ increases with T. For sufficiently large T, the profile with T converges to a "limiting" straight line, which can be found from Eqs. (32) and (33) under the condition that $T\to\infty$. For the coercive field E_c of the sample, the effect of E_c on D_{off}(sat) is shown in Fig. 11 with different

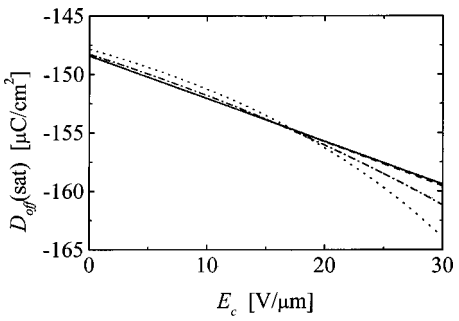

FIG. 11. The variation of D_{off} with the coercive field E_c of the sample. The solid, dashed, dash-dotted, and dotted lines denote the period $T=0.1$ s, 10 s, 100 s, and 200 s, respectively.

periods T of the applied field. It is clear that the magnitude of D_{off}(sat) increases as E_c increases, and such behavior of D_{off}(sat) is described by Eqs. (32) and (33). We have found that E_A^+(sat) increases when we increase E_c. Thus, a larger magnitude of D_{off}(sat) is observed. With small enough E_c, the magnitude of D_{off}(sat) decreases monotonically with T. As E_c continuously increases, it is seen that the increment of $|D_{off}(\text{sat})|$ with the largest T is fastest. There is a critical value of E_c beyond which this trend is reversed (about 17 V/μm in our case). Interestingly, when T is sufficiently small, the increment of $|D_{off}(\text{sat})|$ with E_c tends to be linear.

Summing up, the most significant point is that a small asymmetry in the electrical conductivity is already sufficient to generate a large polarization offset. In agreement with the views of Poullain *et al.*[29] and Bouregba *et al.*,[30] electrical conductivity in the ferroelectric film material should have an important role to play. Previously, we have demonstrated the significance of conductivity to understand some interesting polarization switching results[37] and in the poling process of ferroelectric composites.[38] It allows charge movement as well as charge accumulation at interfaces under field excitation. This work seems to affirm that such consideration may also be essential for discussing the effect of polarization offset, especially for dynamic response.

Our analytical formulation is also suitable for the study of the behavior of other ferroelectric layered structures. For example, by using proper boundary conditions our current formalism may be extended to study the hysteresis behavior of ferroparaelectric superlattices.[39]

IV. CONCLUSIONS

In conclusion, the use of a parallelogramlike P_f-E_f loop allows us to obtain explicit expressions for the time development and the final hysteresis loop of ferroelectric films with symmetric and asymmetric conductivities. The resistive loss can be significant for high conductivity film, especially for low frequency measurement. On the other hand, it is shown that a small asymmetry in the electrical conductivities is already sufficient to generate a large polarization offset in the D-E measurement, almost irrespective of high or low resistivity values. This suggests that the gradient introduced by the graded ferroelectrics generates a large asymmetry in conductivities, even though the films possess only low conductivity as reported. Moreover, high permittivity of film, high capacity of reference capacitor, and large amplitude of applied field will also greatly enhance the effect of polarization offset. As have also been noted in some published experimental works, our derived expressions affirm that the time development of the polarization offset shows an exponential (increasing/decreasing) variation with time. All in all, many qualitative features of previous experimental results are reproduced by our predictions.

ACKNOWLEDGMENT

This work was partially supported by the Center for Smart Materials of The Hong Kong Polytechnic University.

[1] C. B. Sawyer and C. H. Tower, Phys. Rev. **35**, 269 (1930).
[2] M. E. Lines and A. M. Glass, *Principles and Applications of Ferroelectrics and Related Materials* (Oxford University, New York, 1977), p. 104.
[3] S. L. Miller, R. D. Nasby, J. R. Schwank, M. S. Rodgers, and P. V. Dressendorfer, J. Appl. Phys. **68**, 6463 (1990).
[4] L. Wu, T. S. Wu, C. C. Wei, and H. C. Liu, J. Phys. C **16**, 2823 (1983).
[5] C. Voisard, D. Damjanovic, and N. Setter, J. Eur. Ceram. Soc. **19**, 1251 (1999).
[6] H. S. Nalwa, *Handbook of Thin Film Materials* (Academic, San Diego, 2002), Vol. 3, Chap. 1.
[7] G. Ornelas-Arciniega and J. Reyes-Gómez, J. Korean Phys. Soc. **32**, S380 (1998).
[8] M. Trybus and W. Proszak, Proc. SPIE **2373**, 347 (1995).
[9] M. Brazier, S. Mansour, E. Paton, and M. Mcelfresh, Integr. Ferroelectr. **18**, 579 (1997).
[10] J. H. Park, B. K. Kim, J. G. Park, I. T. Kim, H. J. Je, Y. Kim, and S. J. Park, Ferroelectrics **230**, 453 (1999).
[11] J. Hatano, T. Watanabe, and R. Lebihan, Ferroelectrics **126**, 311 (1992).
[12] R. Bouregba and G. Poullain, Ferroelectrics **274**, 165 (2002).
[13] J. J. Lee and S. B. Desu, Ferroelectr. Lett. Sect. **20**, 27 (1995).
[14] E. G. Lee and S. J. Kim, J. Korean Phys. Soc. **42**, 158 (2003).
[15] L. Zheng, C. Lin, W.-P. Xu, and M. Okuyama, J. Appl. Phys. **79**, 8634 (1996).
[16] A. Furuya and J. D. Cuchiaro, J. Appl. Phys. **84**, 6788 (1998).
[17] Y.-I. Kim and W. J. Lee, Jpn. J. Appl. Phys., Part 1 **39**, 1309 (2000).
[18] K. W. Lee, Y. I. Kim, and W. J. Lee, Ferroelectrics **271**, 1769 (2002).
[19] T. Lü and W. Cao, Microelectron. Eng. **66**, 818 (2003).
[20] C. L. Wang, L. Zhang, Y. P. Peng, W. L. Zhong, P. L. Zhang, and Y. X. Wang, Solid State Commun. **109**, 213 (1999).
[21] K. Abe, N. Yanase, T. Yasumoto, and T. Kawakubo, Jpn. J. Appl. Phys., Part 1 **41**, 6065 (2002).
[22] L. Zheng, C. Lin, and T.-P. Ma, J. Phys. D **29**, 457 (1996).
[23] L. Zheng, C. Lin, and M. Okuyama, J. Phys. D **29**, 2020 (1996).
[24] P. Yang, D. L. Carroll, J. Ballato, and R. W. Schwartz, Appl. Phys. Lett. **81**, 4583 (2002).
[25] J. Rodríguez Contreras, H. Kohlstedt, U. Poppe, R. Waser, C. Buchal, and N. A. Pertsev, Appl. Phys. Lett. **83**, 4595 (2003).
[26] P. W. M. Blom, R. M. Wolf, J. F. M. Cillessen, and M. P. C. M. Krijn, Phys. Rev. Lett. **73**, 2107 (1994).
[27] Y. Watanabe, D. Sawamura, and M. Okano, Solid State Ionics **108**, 109 (1998).
[28] C. Yoshida, A. Yoshida, and H. Tamura, Appl. Phys. Lett. **75**, 1449 (1999).
[29] G. Poullain, R. Bouregba, B. Vilquin, G. Le Rhun, and H. Murray, Appl. Phys. Lett. **81**, 5015 (2002).
[30] R. Bouregba, G. Poullain, B. Vilquin, and G. Le Rhun, J. Appl. Phys. **93**, 5583 (2003).
[31] T. Kanashima and M. Okuuama, Jpn. J. Appl. Phys., Part 1 **38**, 2044 (1999).
[32] T. Hauke, R. Steinhausen, W. Seifert, H. Beige, and M. Kamlah, J. Appl. Phys. **89**, 5040 (2001).
[33] J. V. Mantese, N. W. Schubring, A. L. Micheli, A. B. Catalan, M. S. Mohammed, R. Naik, and G. W. Auner, Appl. Phys. Lett. **71**, 2047 (1997).
[34] M. Brazier, M. McElfresh, and S. Mansour, Appl. Phys. Lett. **72**, 1121 (1998).
[35] D. Bao, X. Yao, and L. Zhang, Appl. Phys. Lett. **76**, 2779 (2000).
[36] M. Brazier, M. McElfresh, and S. Mansour, Appl. Phys. Lett. **74**, 299 (1999).
[37] C. K. Wong, Y. W. Wong, and F. G. Shin, J. Appl. Phys. **92**, 3974 (2002).
[38] Y. T. Or, C. K. Wong, B. Ploss, and F. G. Shin, J. Appl. Phys. **93**, 4112 (2003).
[39] V. A. Stephanovich, I. A. Luk'yanchuk, and M. G. Karkut, Ferroelectrics **291**, 385 (2003).